Proceedings of the 21st ICSMGE, Vienna, Austria, 14 – 19 June 2026. Pistrol, Adam & Schweiger (eds.)
Published by: ÖGG, Austrian Society for Geomechanics, Salzburg, Austria, ISBN 978-3-9503898-4-5
https://doi.org/10.53243/ICSMGE2026-1676

Effectiveness of equivalent linear approach for analyzing tunnel-pipeline interaction

Tomasz Durjasz
Tunnel Engineer, Ramboll, Denmark, tomd@ramboll.dk

Assaf Klar
Faculty of Civil and Environmental Engineering, Technion-Israel Institute of Technology, Israel, klar@technion.ac.il

Varvara Zania
Department of Environmental and Resource Engineering, DTU, Denmark, vaza@dtu.dk

ABSTRACT: The expansion of urban infrastructure demands robust assessment methodologies to manage risks associated with tunneling near existing underground utilities. This research presents a parametric study using the Design Oriented Linear Equivalent Approach (DOLEA) to examine interactions between tunnel-induced soil displacements and adjacent buried pipelines. The DOLEA method utilizes an elastic-continuum analysis coupled with iterative calculations of equivalent stiffness to address soil nonlinearity, providing a comprehensive tool for soil-pipeline interaction assessment. The study evaluates the effectiveness of DOLEA through comparisons with a parametrically varied 3D Finite Element Model (FEM). This analysis focuses on varying tunnel parameters, pipeline characteristics, and soil conditions while covering a wide range of tunnel-induced volume losses. Additionally, the study investigates pipeline responses under both the Hardening Soil model and the Hardening Soil Small model to determine their applicability in different soil behavior scenarios. Validation of the FEM models was conducted using data from centrifuge tests.

KEYWORDS: Tunnel-pipeline interaction, Equivalent linear method, Soil-structure interaction, Ground settlement, Finite element modeling, Hardening soil model, Urban tunneling, Parametric study

1 INTRODUCTION

Global urbanization has led to an increased demand for utilization of the underground space, where tunnels are one the central solutions for expanding transportation infrastructure. Tunneling, however, can pose challenges to existing buildings and aging buried infrastructure, such as pipelines. Tunnel-induced settlements can affect buried pipelines and risk being damaged or even destroyed by large settlements, leading to safety hazards and costly repairs. Therefore, a better understanding of how tunneling impacts overlying infrastructure and the associated risks is crucial.

Early approaches to tunnel-pipeline interaction relied on Winkler-type models, where the soil was modeled as linear springs reacting independently to pipeline displacement (Attewell et al., 1986). While computationally efficient, these models oversimplified soil-structure interaction and ignored the influence of shear strain and stiffness degradation.

Elastic-continuum approaches were developed by Klar et al. (2005) for continuous pipelines and by Klar et al. (2008) for jointed pipelines, offering better representations of soil continuity and stress distribution. These methods enabled closed-form solutions for pipeline bending moments due to tunneling-induced settlements (and later were validating your Fourier based exact solutions, Klar (2018, 2022).

Vorster et al. (2005) introduced an equivalent linear approach, incorporating strain-dependent stiffness based on estimated shear strains derived from greenfield displacements. This approach was later refined by Marshall et al. (2010), who, using centrifuge tests and PIV, showed that out-of-plane shear components significantly influence pipeline response and should be included in strain estimation for accurate stiffness selection.

The Design Oriented Linear Equivalent Approach (DOLEA), developed by Klar et al. (2016), synthesizes key advances in tunnel-pipeline interaction, such as elastic-continuum solutions and observations from centrifuge tests, into a practical, iterative framework. It employs a set of equations within a linear-equivalent approach that accounts for soil nonlinearity. Using greenfield settlement profiles as input, DOLEA estimates pipeline response. The method has been validated against centrifuge experiments and Discrete Element Method (DEM) simulations, showing good agreement across a range of tunnel volume losses and pipeline stiffness values.

Finite element analysis (FEA) is also a widely used tool used to assess the risks posed by tunneling to buried infrastructure. However, creation of detailed FEM models can be time-consuming, computationally expensive, and often require complex constitutive models to represent the problem accurately, defining the soil parameters can also be challenging (Mair and Taylor, 1999). The design-oriented linear equivalent approach (DOLEA), proposed by Klar et al. (2016), offers an alternative tool addressing the problem.

The aim of this paper is to evaluate the effectiveness of DOLEA for tunneling beneath pipelines in dense unsaturated sands in wide range of tunnel and pipe parameters (in the original paper the validation was carried out for one tunnel diameter of 4.65 m with axis at depth 13.65 m). Through a parametric study, DOLEA predictions are compared against pipeline response in the 3D FEM models under varying tunnel depths, diameters, and pipe stiffnesses. Two advanced constitutive are used: Hardening Soil (HS) and Hardening Soil Small (HSsmall). The numerical models are validated against centrifuge test data, ensuring the credibility of the simulations and analytical approach.

2 METHODOLOGY

PLAXIS 2D (version 2024.2) was used to develop a plane strain model under greenfield conditions. This model provided the settlement profile required as input for calculating the maximum pipeline bending moment (M_{max}) using the DOLEA approach (further described in subsection 2.6). PLAXIS 3D (version 2024.2) was then used to construct a 3D model including both the tunnel and the pipeline, serving as the basis for comparison between the DOLEA-predicted M_{max} and the maximum moment obtained directly from the 3D finite element simulation.

To ensure the FE results were a valid basis for comparison, the modeling approach was first validated against experimental data to assess its accuracy in predicting ground and pipeline responses.

2.1 *Model validation*

The 2D finite element model is validated by replicating the centrifuge experiment conducted by Franza et al. (2019), which examined the behavior of dense Leighton Buzzard Sand under greenfield conditions with a cover-to-diameter (C/D) ratio of 2.44 and a centrifugal acceleration of 75 g. Validation focused on comparing the FEM results against experimental observations for volume loss versus surface settlement, maximum vertical displacement, and internal tunnel pressure.

Lanzano et al. (2016) provided input parameters for Leighton buzzard Sand for HS and HSs models for relative density of 75%, which differs from the 90% relative density used in the centrifuge tests. The small-strain stiffness values reported appear lower than those presented in Cavallaro et al. (2001), with discrepancies reaching up to 50%. To address this, a targeted calibration of the stiffness parameters for both the HS and HSsmall models was carried out to reflect the behavior of Leighton Buzzard Sand at 90% relative density.

The calibration process was performed in PLAXIS SoilTest optimization tool, using drained triaxial compression test data from Lanzano et al. (2016). Stiffness parameters E_{50}, E_{oed}, E_{ur} were adjusted to best match triaxial tests, while all remaining input parameters were derived based on the empirical relationships provided by Brinkgreve et al. (2010).

Table 1. HS and HSsmall model parameters dense sands for calibration.

Parameter	Symbol	Value	Unit
Relative Density	I_D	90	%
Unit Weight Unsaturated	γ_{unsat}	18.6	kN/m^3
Young's modulus	E_{50}	33	MPa
Oedometer modulus	E_{oed}	33	MPa
Unloading/reloading modulus	E_{ur}	66	MPa
Small-strain shear modulus	$G_{0,ref}$	121.2	MPa
Reference strain at 0.7 G_0	$\gamma_{0.7}$	1.1E-04	-
Power for stiffness increase	m	0.42	-
Friction angle	ϕ	39.3	°
Dilatancy angle	ψ	9.3	°
Failure ratio	R_f	0.89	-
Poisson's ratio	v	0.3	-

Following this calibration a centrifuge model was developed using PLAXIS 2D to validate the numerical approach against experimental test data from Franza et al. (2019). The model dimensions were matched to the rigid container used in the Nottingham centrifuge facility (770 mm × 311 mm). The lateral boundaries were normally fixed, the bottom was fully restrained, and the top surface was free. The pressurized latex membrane used in the centrifuge test was modeled by applying a circular outward radial line load, This load was defined by a reference pressure at the tunnel axis level and an incremental pressure variation with depth, calculated using the unit weight of water and the expected vertical soil stress at that depth.

Centrifuge-induced gravity loading was simulated by increasing the self-weight multiplier in PLAXIS to match the 75g field acceleration used in the experiment. The progressing volume loss was modeled by stepwise reduction of the internal line load within the tunnel cavity, simulating depressurization due to water extraction. This procedure induced settlement and shear strains in the surrounding soil, analogous to the physical centrifuge test conditions.

The simulation process consisted of three stages: (1) an initial stress generation stage using the K_0 procedure under 1g conditions, (2) a spin-up stage applying 75g acceleration and activating the tunnel load to balance in-situ vertical stresses, and (3) progressive volume loss stages achieved through incremental load reduction.

2.2 *2D Greenfield Model*

The prototype-scale 2D model was created in PLAXIS 2D using the same modeling principles as the centrifuge validation setup but scaled to full prototype dimensions. The boundary conditions are consistent with the earlier model. However, unlike the centrifuge case, gravity is maintained at 1g.

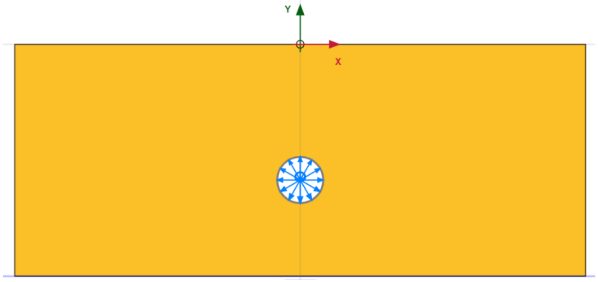

Figure 1. PLAXIS 2D model of the centrifuge test with greenfield conditions.

To minimize boundary effects and ensure numerical accuracy, the model boundaries are extended beyond those used in the centrifuge simulation. This extension is essential for the subsequent parametric study, which involves varying tunnel depth and diameter. The boundary dimensions are selected based on empirical recommendations from Möller (2006), who proposed guidelines for finite element modeling of tunnel problems in both 2D and 3D. These guidelines define the lateral boundary distance from the tunnel axis as a function of tunnel diameter and cover-to-diameter ratio (C/D_t), expressed by:

$$l = D_t \cdot \left(12 + \frac{13}{3} \cdot \frac{C}{D_t}\right) \quad (1)$$

Additionally, to control vertical boundary effects, the distance from the tunnel invert to the bottom boundary is set to 1.4 times the tunnel diameter. This value falls within the recommended range of 1.3 to 2.2 times the diameter for tunnels between 4 m and 12 m.

2.3 *3D Model with pipeline*

To simulate tunnel-pipeline interaction at prototype scale, a 3D model was developed using PLAXIS 3D. The model replicates real-world geometry and operates under standard gravity (1g). Boundary conditions mirror those of the 2D model.

The buried pipeline is represented by a fully-elastic plate element extending across the model width, while the tunnel is simulated using a cylindrical surface subjected to a surface load, which is incrementally reduced to replicate volume loss.

The vertical dimension from tunnel invert to the model base is set to 1.4 times the tunnel diameter, in line with the 1.1-1.45 range recommended by Möller (2006) to minimize boundary influence. While Möller also provides a guideline for model length based on longitudinal settlement profiles during staged excavation, this study simplifies tunnel construction by modeling only volume loss. Therefore, the model length is set to 20 times the pipeline diameter.

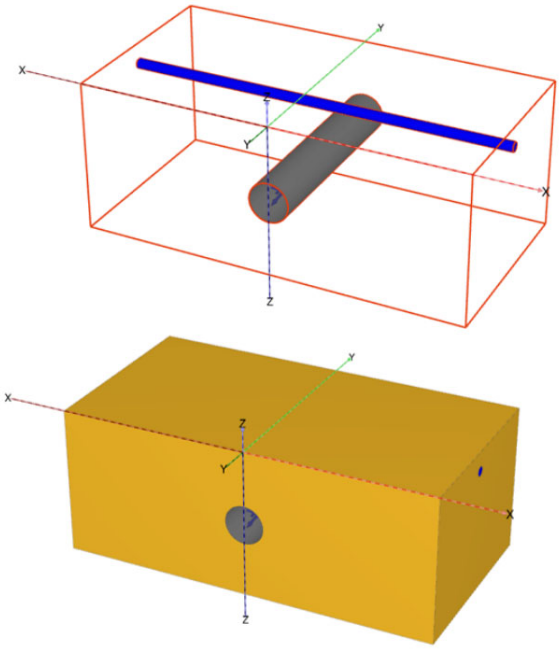

Figure 2. PLAXIS 3D full-scale model test with buried pipeline.

The modeling sequence includes four stages. First, the initial stress state is established using the K_0 procedure under 1g. Second, the tunnel is installed by deactivating the tunnel soil cluster and activating a balancing tunnel-surface load that counteracts vertical stress at tunnel axis level. Third, the pipeline is introduced by deactivating the surrounding soil and activating the plate elements. Finally, volume loss is simulated through a series of progressive load reductions.

Although pipelines are generally installed prior to tunnelling in practice, the sequence is reversed in this model to prevent artificial moment generation during pipeline activation. To ensure accurate simulation of initial conditions, all strains, state variables, and displacements are reset after the tunnel installation stage.

2.4 *Parametric Study*

Three tunnel diameters (5.0 m, 6.7 m, and 9.3 m) and three depths (13 m, 18 m, and 24 m) are considered in the study, resulting in cover-to-diameter (C/D) ratios ranging from 1.4 to 4.3. Seven tunnel configurations are examined to capture both shallow and deep tunneling effects. The parameters of the considered tunnels are presented in Table 2.

Table 2. Tunnel parameters employed for the parametric study.

Scenario	D_t	Z_t	C/D_t
T1D1	5.0	13.0	2.10
T1D2	5.0	18.0	3.10
T1D3	5.0	24.0	4.30
T2D2	6.7	18.0	2.19
T2D3	6.7	24.0	3.08
T3D2	9.3	18.0	1.44
T3D3	9.3	24.0	2.08

Three pipeline types with varying diameters (610 mm, 1626 mm, and 2235 mm) and stiffness levels are selected for the parametric study, based on commercial steel pipe specifications. Each pipe is considered with two wall thicknesses to evaluate the impact of flexural rigidity, resulting in a wide stiffness range. The resulting range of H/D_t ratio (H - soil thickness between tunnel crown and pipeline invert) is between 0.8 and 3.6. The summary of the considered pipeline parameters are presented in Table 3.

Table 3. Pipeline parameters employed for the parametric study.

Pipe type	D_p	Z_p	EI [kNm^2]
P1S1	0.610	3.0	1.09E+05
P1S2	0.610	3.0	2.86E+05
P2S1	1.626	3.8	4.12E+06
P2S2	1.626	3.8	8.06E+06
P3S1	2.235	5.0	6.94E+06
P3S2	2.235	5.0	2.12E+07

The parametric study varied tunnel geometry (diameter and depth) and pipeline characteristics (diameter and flexural stiffness) in combination. For each of the seven tunnel configurations listed in Table 2, all six pipeline configurations in Table 3 were analyzed. This allowed assessment of tunnel–pipeline interaction across a broad spectrum of C/D_t ratios and stiffness contrasts.

2.5 *Sand parameters for the parametric study*

Loose and Dense unsaturated sands are considered for the parametric study. The corresponding HS and HSs parameters were defined according to empirical relationships by Brinkgreve et al. (2010). The parameters are presented in Table 4.

Table 4. HS and HSsmall model parameters sands

Parameter	**Symbol**	**Loose**	**Dense**	**Unit**
Relative Density	I_D	30	90	%
Unit Weight Unsaturated	γ_{unsat}	16.2	18.6	kN/m^3
Young's modulus	E_{50}	18	54	MPa
Oedometer modulus	E_{oed}	18	54	MPa
Unloading/reloading modulus	E_{ur}	54	162	MPa
Small-strain shear modulus	$G_{0,ref}$	80.4	121.2	MPa
Reference strain at 0.7 G_0	$\gamma_{0.7}$	1.7E-4	1.1E-04	-
Power for stiffness increase	m	0.6	0.42	-
Friction angle	ϕ	31.75	39.3	°
Dilatancy angle	ψ	1.25	9.23	°
Failure ratio	R_f	0.96	0.89	-
Poisson's ratio	v	0.3	0.3	-

2.6 *DOLEA*

The Design Oriented Linear Equivalent Approach (DOLEA) is implemented to estimate the maximum bending moment induced in a buried pipeline due to tunnel-induced ground movements M_{max}.

First step is determination of the greenfield displacement profile along with its modified Gaussian parameters: S_{max}, i and n. For that input, the settlement profile is extracted from the 2D PLAXIS model at the level where the pipeline is expected. The settlement trough is fitted using a modified Gaussian function:

$$S_v(x)\frac{n}{(n-1)+exp\left(\alpha\frac{x^2}{i^2}\right)}\cdot S_{max} \qquad (2)$$

$$n = e^{\alpha}\cdot\frac{2\alpha-1}{2\alpha+1}+1$$

The fitting is optimized through the curve fit function from the scipy.optimize Python package.

Next step is calculation of the associated shear strains and out-of-plane shear strains, calculated employing equation 2 with fitted polynomial expressions according to Figure 3:

$$\gamma_a = \left[x_1 + x_2 \cdot \frac{i^2}{(z_t - z_p)^2} - x_3 \cdot \frac{i}{z_t - z_p} C \right] \frac{s_{max}}{i} \quad (3)$$

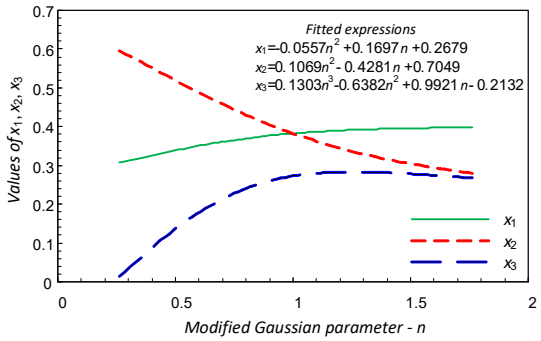

Figure 3. Fitted polynomial expressions used for calculating the shear strains from Klar et al. (2016).

Next step is to determine the equivalent shear strain:

$$\gamma_{eq} = \sqrt{\gamma_a^2 + \gamma_j^2} \quad (4)$$

where setting γ_j equal to 0 during the initial iteration and for next iterations:

$$\gamma_j = 1.3 \frac{\delta_r}{r_0} = 1.3 \frac{\left[1 - \Lambda\left(\frac{M_{max}}{M_{\max,gf}}\right)\right] s_{max}}{r_0} = \\ = 0.39 \left(\frac{M_{max}}{M_{\max,gf}}\right)^{0.115} \ln\left(\frac{M_{max}}{M_{\max,gf}}\right) \frac{s_{\max}}{r_0} \quad (5)$$

Next, the secant Young's modulus E_s is obtained by applying a nonlinear relationship or backbone curve based on the equivalent shear strain obtained from previous step.

For models using the Hardening Soil (HS) constitutive model, stiffness degradation is based on the strain-dependent reduction derived from a hyperbolic stiffness-strain relationship:

$$q = \frac{\varepsilon_1}{\frac{1}{2E_{50}} + \frac{\varepsilon_1 R_f}{q_f}} \quad (6)$$

where ε_1 is the principal strain, q is the deviatoric stress, E_{50} is stiffness at mobilization of 50% of the maximum shear strength, q_f is the ultimate deviatoric stress.

For the Hardening Soil Small-Strain (HSsmall) model, the degradation is defined through the parameter $\gamma_{0.7}$ (shear strain at which the shear modulus is reduced by 70 % of its initial value) using the Santos and Correia (2001) formulation:

$$\frac{G_s}{G_0} = \frac{1}{1 + 0.385 \left|\frac{\gamma}{\gamma_{0.7}}\right|} \quad (7)$$

Following that, the rigidity factor R is computed with the flexural stiffness of the pipe and the modified gaussian parameters initially fitted to the greenfield settlements curve:

$$R = \frac{EI}{i^3 r_0 E_s} \quad (8)$$

Next step is to determine of the moment ratio:

$$\frac{M_{max}}{M_{\max,gf}} = \frac{1}{1 + 1.1 \frac{\alpha}{n} f_i (f_d R)^{2/3}} \quad (9)$$

where:

$$f_d = \left(1 + 0.93 z_p / r_0\right) / \left(1.07 z_p / r_0\right)$$

$$f_i = 2.18 (i / r_0)^{-1/3}$$

where (r_0) is the pipeline radius.

After completing this step, the iterative process begins by repeating the previous steps, starting with the recalculation of equivalent shear strain using the updated γ_j. The iteration continues until convergence is achieved for both γ_{eq} and R parameters.

The primary output of the procedure is the maximum bending moment, calculated by multiplying the moment ratio obtained from Equation 9 by the moment induced in the pipeline if it was to follow the greenfield displacement curve:

$$M_{\max,gf} = EI \frac{2\alpha}{n} \frac{s_{max}}{i^2} \quad (10)$$

2.7 *Automation*

The setup of the PLAXIS 2D and 3D models was facilitated through Python API scripting, which enabled automation of both the model generation and the intermediate steps of result extraction and post-processing. Figure 4 summarizes the full workflow used in this study, beginning with the generation of greenfield settlements from the 2D FE model, followed by DOLEA moment calculation using the settlement data and the stiffness degradation curve, and parallel 3D FE modelling of tunnel–pipeline interaction. This workflow is repeated for each scenario described in Section 2.4.

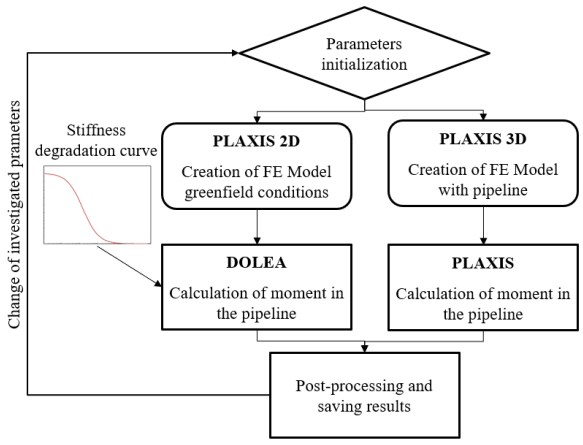

Figure 4. Flowchart of the Python code setup.

3 RESULTS

When compared to the experiments documented by Franza et al. (2019) (see Figure 5), the pressure response of the HS model shows identical behavior up to a $V_{l,t}$ of 0.5% and overpredicts

the asymptote that indicates failure. The agreement of maximum settlements was notably accurate for both the HS and HSsmall models. In terms of volume loss from settlements ($V_{l,s}$) the HSsmall model performed better at half the tunnel depth, but underpredicted $V_{l,s}$ at the surface. Conversely, the HS model accurately predicted $V_{l,s}$ at the surface for tunnel volume losses up to 1.7%.

The tunnel pressure-volume loss relationship reveals that the HSsmall model produced a significantly stiffer response. The results for HS and HSsmall displayed identical maximum settlement depths. However, for $V_{l,s}$ at the surface and half the tunnel depth, the responses were similar for $V_{l,t}$ up to approximately 1%. Beyond this, the $V_{l,s}$ was lower for the HSsmall, indicating a narrower settlement trough compared to the other models.

3.1 *Model validation*

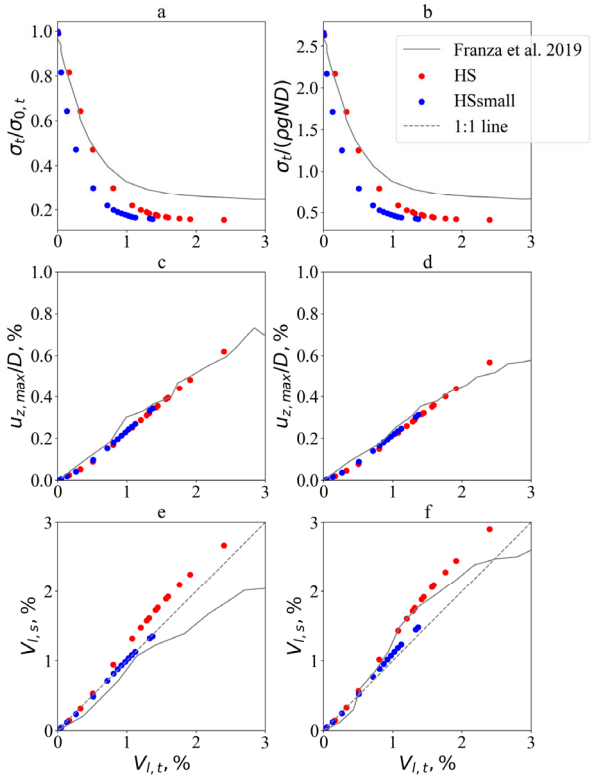

Figure 5. Results for model validation. a) Relative tunnel pressure, b) Normalised tunnel pressure, Variation of normalized maximum settlement for c) $Z/Z_t = 0.5$ and d) $Z/Z_t = 0$, And $V_{l,t}$ vs $V_{l,t}$ for e) $Z/Z_t = 0.5$ and f) $Z/Z_t = 0$.

3.2 *Parametric study – with buried pipeline*

3.2.1 *Dense sands*

The comparison of maximum bending moments induced in the pipeline in dense sand, as predicted by PLAXIS 3D and DOLEA, is shown in Figure 6 (a – Hardening Soil; b – Hardening Soil Small). The grey line represents a 1:1 agreement between the two methods. The red lines above and below the grey line indicate the bounds of a 2:1 and 1:2 ratio, respectively, between the PLAXIS and DOLEA predictions. The focus in this analysis will be made on cases where induced maximum moment in the pipeline is higher than 10kNm.

DOLEA yielded lower pipeline moments than PLAXIS 3D for scenarios T3D2, T1D1, T2D2, and T3D3 at volume losses >1%. These cases correspond to pipelines positioned closest to the tunnel, with H/D_t ratios up to approximately 1.7. Explanation about the effect of the tunnel on the interaction response, leading to higher bending moment, is explained in Klar et al. (2024).

Both the Hardening Soil (HS) and Hardening Soil Small-Strain (HSs) models exhibit similar trends across corresponding scenarios.

It can be observed that for some scenarios, data points at higher volume losses are missing. This is because certain models did not reach the intended volume loss levels due to either numerical failure or insufficient reduction in tunnel pressure across the defined calculation phases.

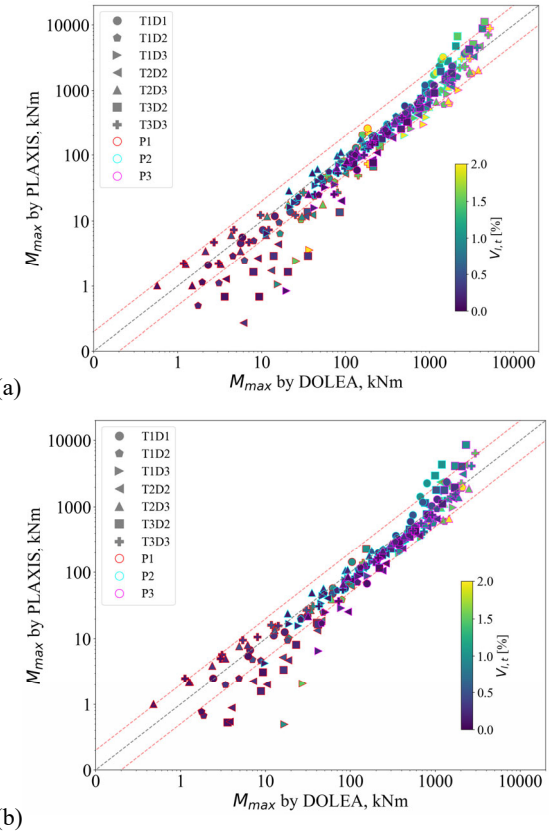

Figure 6. Comparison between results from the DOLEA and 3D PLAXIS for dense sands using a) HS model, b) HSs model.

3.2.2 *Loose sands*

For loose sands (see Figure 7), DOLEA predicts smaller moments than PLAXIS 3D for scenarios T3D3 and T2D3 at low volume losses (<0.3%) and for T3D2 at high volume losses (>1.3%). Similar to the dense sand results, these cases correspond to pipelines positioned closest to the tunnel.

4 SUMMARY AND CONCLUSIONS

The behavior of the 2D finite element PLAXIS model of the centrifuge test was found to be in good agreement with the centrifuge test results. The applied boundary conditions simulated tunnel volume loss by gradually reducing the pressure within the tunnel cluster, as both models adopted a simplified "wished-in-place" approach.

A parametric study was performed for a wide range of tunnel and pipeline parameters (depth and diameter) in unsaturated (dry) dense and loose sands to compare the maximum bending moments induced in the pipeline with decreasing volume loss, using PLAXIS 3D and the Design Oriented Linear Equivalent Approach (DOLEA). PLAXIS 3D used the same methodology as the validated 2D model, with the pipeline represented as a fully elastic plate element.

DOLEA provided similar results to PLAXIS 3D for both HS and HSs models across the studied H/D_t (H – distance between pipe invert and tunnel crown, D_t – tunnel diameter) ratios from 1.7 to 3.6. The method generally yielded similar or more conservative predictions compared to PLAXIS. However, for H/D_t values below 1.7, DOLEA tended to yield smaller maximum moments compared to PLAXIS. This is most likely due to the interaction between the pipeline and the tunnel itself, as explained in Klar et al. (2024).

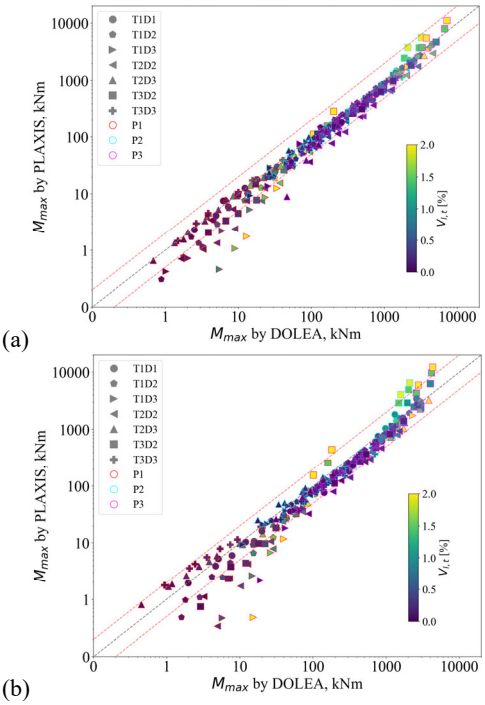

Figure 7. Comparison between results from the DOLEA and 3D PLAXIS for loose sands using a) HS model, b) HSs model.

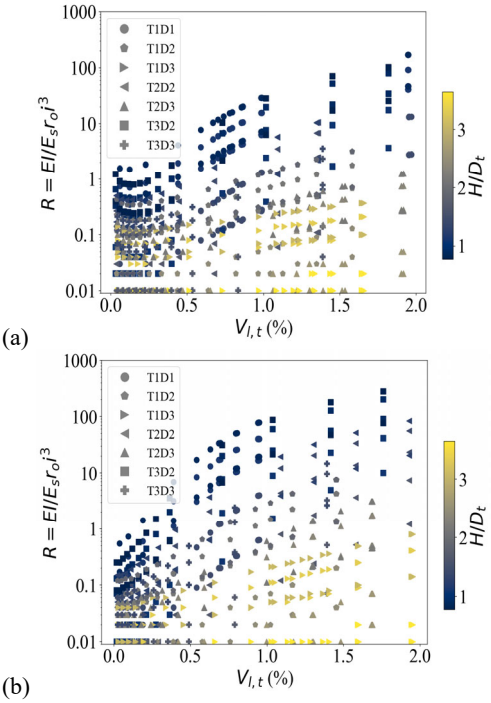

Figure 8. Comparison of R parameter with progressing volume loss for different H/D_t ratios: a) HS model, b) HSs model.

According to Marshall et al. (2010), the parameter R is referred to as a "rigidity" parameter that indicates the level of soil-pipe interaction. In Figure 8, the resulting R is plotted for the investigated scenarios against the tunnel volume loss $V_{l,t}$ with the color map showing the corresponding H/D_t ratio. The graph shows that the closer the tunnel is to the pipeline, the higher the soil-pipe interaction. As mentioned earlier, DOLEA gave lower results than PLAXIS 3D for scenarios where H/D_t was below 1.7. From Figure 8, for cases with H/D_t lower than 1.7, the rigidity factor R is generally higher than 5 for volume losses above 0.5%, indicating high soil-pipeline interaction. This suggests that DOLEA predictions for maximum bending moments may differ from PLAXIS 3D when the pipeline is close to the tunnel and soil-pipeline-tunnel interaction is high.

5 ACKNOWLEDGEMENT

The second author would like to acknowledge the financial support of Israel Science Foundation (grant no. 1425/23).

6 REFERENCES

Attewell, P., Yeates, J., and Selby, A. (1986). Soil movements induced by tunneling and their effects on pipelines and structures.

Brinkgreve, R.B.J., Engin, E., and Engin, HK. (2010). Validation of empirical formulas to derive model parameters for sands. In T. Benz, and S. Nordal (Eds.), *Numerical methods in geotechnical engineering Numge 2010* (pp. 137-142). CRC Press.

Cavallaro, A., Maugeri, M. and Mazzarella, R. (2001). Static and Dynamic Properties of Leighton Buzzard Sand from Laboratory Tests.

Franza, A., Marshall, A.M. and Zhou, B. (2019). Greenfield tunnelling in sands: the effects of soil density and relative depth. In: Géotechnique 69, pp. 297—307.

Klar, A., Vorster, T. E. B., Soga, K., and Mair, R. J. (2005). Soil-pipe interaction due to tunneling: Comparison between Winkler and elastic-continuum solutions. Géotechnique, 55(6), 461–466.Klar, A. (2018). Elastic Continuum Solution for Tunneling Effects on Buried Pipelines Using Fourier Expansion. *Journal of Geotechnical and Geoenvironmental Engineering*, *144*(9), 1–10. https://doi.org/10.1061/(ASCE)GT.1943-5606.0001945

Klar, A. (2022). A Fourier-based elastic continuum solution for jointed pipeline response to tunneling. *Tunnelling and Underground Space Technology*, *119*, 104237.

Klar, A., Elkayam, I., and Marshall, A. M. (2016). Design Oriented Linear-Equivalent Approach for Evaluating the Effect of Tunneling on Pipelines. J. Geotech. Geoenviron. Eng., 142(8).

Klar, A., Franza, A., Zhou, M., and Huang, H. (2024). Introducing tunnel kinematic constraints into an elastic continuum formulation of tunnel-soil-pipeline interaction. *Geotechnique,* https://doi.org/10.1680/jgeot.24.00023

Klar, A., Marshall, A. M., Soga, K., and Mair, R. J. (2008). Tunneling effects on jointed pipelines. *Canadian Geotechnical Journal*, *45*(1), 131–139.

Klar, A., Vorster, T. E. B., Soga, K., and Mair, R. J. (2005). Soil-pipe interaction due to tunneling: Comparison between Winkler and elastic-continuum solutions. Géotechnique, 55(6), 461–466.

Mair, R. J. and Taylor, R. N. (1999). Theme lecture: Bored tunnelling in the urban environment. In 14th International conference on soil mechanics and foundation engineering, pages 2353 – 2385.(Hamburg, Balkema). Jan 1999.

Marshall, A. M., Klar, A., and Mair, R. J. (2010b). Tunneling beneath buried pipes: A view of soil strain and its effect on pipeline behavior. J. Geotech. Geoenviron. Eng., 136(12), 1664–1672.

Möller, S.C. (2006). Tunnel induced settlements and structural forces in linings. Univ. Stuttgart, Inst für Geotechnik Stuttgart, Germany, 2006.

Peck, R. B. (1969). Deep excavations and tunneling in soft ground. 7th ICSMFE.

Santos, J.A. and Correia, A.G, (2001) Reference threshold shear strain of soil. 15th International Conference on Soil Mechanics and Geotechnical Engineering.

Vorster, E. Klar, A., Soga, K., and Mair, R. (2005). Estimating the Effects of Tunneling on Existing Pipelines. Journal of Geotechnical and Geoenvironmental Engineering. 131.